# Supporting information

## A simple, versatile and robust centrifugation-based filtration protocol for the isolation and quantification of α-synuclein monomers, oligomers and fibrils: towards improving experimental reproducibility in α-synuclein research

Senthil T. Kumar[1], Sonia Donzelli[1], Anass Chiki[1], Muhammed Muazzam Kamil Syed[1] & Hilal A. Lashuel*[1]

[1]Laboratory of Molecular and Chemical Biology of Neurodegeneration, Brain Mind Institute, EPFL, Switzerland

**Table of contents**

## Supplementary tables

**Supplementary table 1** Common centrifugal parameters used to prepare different aSyn species.

| aSyn species | Centrifugal parameters | Rationale | References |
|---|---|---|---|
| WT, A30P, or A53T monomers | 50 µl aliquot at 16000*g* for 5 min | To remove insoluble material using a benchtop centrifuge | Conway *et al.* 2000 |
| WT aSyn fibrils | 90-µl aliquot at 40000*g* for 30 min | To measure the amount of fibril pellet remaining during fibril disassembly | Bousset *et al.* 2013 |
| aSyn 30–110 fibrils | 16000*g* for 30 min | To monitor fibril disassembly when co-incubated with chaperones | Gao *et al.* 2015 |
| Labeled aSyn fibrils | 15000*g* for 10 min | To remove the free fluorophores after the labeling of fibrils | Fenyi *et al.* 2018 |
| aSyn strain A and B PFFs | 100000*g* for 15 min | Seeds were resuspended in $D_2O$ for structural studies | Guo *et al.* 2013 |
| WT aSyn PFFs | 100000*g* for 30 min | Sedimentation assay for confirmation of pelletable, active PFFs for cellular assays | Volpicelli-Daley *et al.* 2014 |
| WT aSyn PFFs | 20000*g* for 10 min | To sediment down PFFs after sonication | Fares *et al.* 2016 |

**Supplementary table 2** Summary of different protocols for the preparation of aSyn oligomers and their structural properties.

| Oligomers | Diameter | Morphology | Size distribution | Methods | References |
|---|---|---|---|---|---|
| WT aSyn | 11 (±1) nm<br><br>13 nm to 17 nm | annular and tubular<br><br>spherical | 600 kDa (>42 monomers)*<br>539 kDa (n=38), 368 kDa (n=26) and 308 kDa (n=21 monomers)#∝ | EM, SEC, SV-AUC and STEM | Lashuel *et al.* 2002 |
| WT aSyn | ~4 nm | spherical | N.A. | SEC and AFM | Volles *et al.* 2001 |
| WT aSyn on-pathway oligomers | ~20 nm | globular | ~140–900 kDa<br>(~10–60 monomers)# | EM and SV-AUC | Pieri *et al.* 2012 |
| WT aSyn dopamine-induced oligomers | 20 - 60 nm | spherical/globular | N.A. | EM and SDS-PAGE analysis | Mahul-Mellier *et al.* 2015 |
| WT aSyn ONE-induced oligomers | 4–8 nm in height and 40–80 nm in width | amorphous round species | ~ 2000 kDa* | SEC and AFM | Näsström *et al.* 2009 |
| WT aSyn HNE-induced oligomers | 2–4 nm in height and 100–200 nm in length<br><br>30–50 nm in inner diameter, 80–100 nm in outer diameter | curved protofibril-like<br><br>annular structures | ~ 2000 kDa* | SEC and AFM | Näsström *et al.* 2011 |
| WT aSyn on-pathway<br><br>DA crosslinked oligomers<br><br>GA crosslinked oligomers | N.A. | N.A. | ~450 kDa (~30 monomers)<br><br>~300 kDa (~20 monomers)<br><br>large: 228 kDa (~16 monomers);<br>medium: 88 kDa (~6 monomers);<br>small: 64 kDa (~4 monomers)#¥ | EM and SV-AUC | Pieri *et al.* 2016 |
| WT aSyn oligomers<br><br>Type A1<br><br>Type A2<br><br>Type B1<br><br>Type B2<br><br>Types C1 and C2 | <br><br>2-45 nm<br><br>2-45 nm<br><br>3-23 nm (height)<br><br>3-23 nm (height)<br><br>4–10 nm (height) | <br><br>spherical and annular<br><br>globular and annular<br><br>spherical<br><br>amorphous<br><br>globular and protofibrillar | N.A. | AFM | Danzer *et al.* 2007 |
| WT aSyn | 3-16 nm (height) | spherical | 160 to 560 kDa (11-39 monomers)# | SEC, AFM, EM and AUC | Chen *et al.* 2015 |
| WT aSyn large oligomers<br><br>small oligomers | ~150–300 nm (length)<br><br>1–2 nm (height) | distinctly elongated<br><br>spherical (disc shaped) | (5.8 ± 3.3) ×10$^3$ kDa<br><br>430 ± 88 kDa$ | SEC-MALLS, EM and AFM | Lorenzen *et al.* 2014 |
| WT aSyn | 20 nm | spherical | N.A. | SEC and EM | Paslawski *et al.* 2016 |

*Based on the SEC of the protofibrils eluted in the void volume compared to the elution volume of protein standards. #Based on SV-AUC analysis. ∝Void volume peak of SEC divided into early, middle and late elutions SV-AUC carried out, respectively. $Based on SEC-MALLS. ¥SV-AUC carried out directly on the on-pathway oligomers formed during the lag phase of fibrillation without any SEC-based isolation. EM: electron microscopy; SEC: size exclusion chromatography; SV-AUC: sedimentation velocity analytical ultracentrifugation; STEM:

scanning transmission electron microscopy; AFM: atomic force microscopy; MALLS: multiple angle laser light scattering; DA: dopamine; GA: glutaraldehyde; ONE: 4-oxo-2-nonenal; HNE: 4-hydroxy-2-nonenal. N.A.: not available.

**Supplementary figures**

Supplementary figure 1

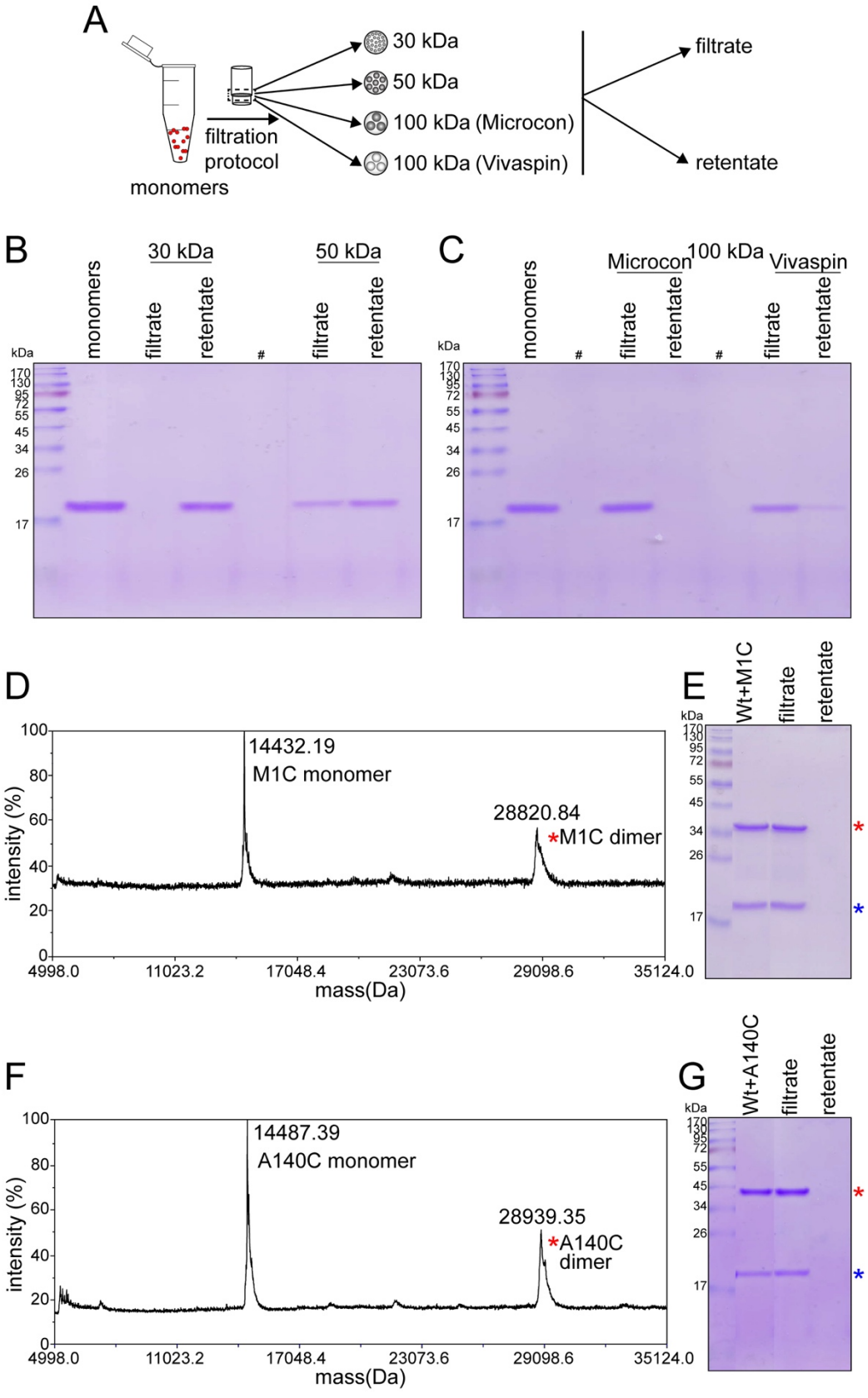

**Supplementary figure 1:** A) Schematic depiction showing the experimental setup used to assess aSyn monomer recovery using three different MWCO membranes - 30 kDa (Microcon), 50 kDa (Microcon) and 100 kDa (from commercial sources, Microcon and Vivaspin). B) SDS-PAGE analysis of the filtrate and retentate samples to assess the efficiency of the recovery of aSyn monomers after passing through 30 kDa, 50 kDa and 100 kDa membranes. C) Assessment of the recovery of aSyn monomers after filteration through a 100 kDa membrane from two different commercial resources, Microcon and Vivaspin. D) and F) Mass spectrometry analysis of M1C-linked (D) and A140C-linked (F) aSyn homodimers. Expected masses for M1C monomer and dimer are 14432 Da and 28864 Da, respectively. Expected masses for A140C monomer and dimer are 14492 Da and 28982 Da, respectively. Observed masses are shown in the figure. E) and G) Assessment of the efficiency of recovery of equimolar mixtures of WT aSyn monomers and disulfide-linked aSyn dimers, M1C (E) or A140C (G), after filtration through a 100 kDa membrane (Microcon). Blue * denotes the WT aSyn monomers and red * denotes the dimeric forms of aSyn cysteine variant M1C and A140C.

To determine which MWCO membrane provides the most efficient separation of aSyn monomers from oligomers, we first assessed and compared monomer recovery using 30 kDa, 50 kDa and 100 kDa MWCO membranes (supplementary fig. 1A). As shown in supplementary fig. 1B, a complete recovery of aSyn monomers into the filtrate fraction was observed only when using a 100 kDa membrane and not a 50 kDa or a 30 kDa membrane. This is consistent with the higher predicted molecular weight of aSyn based on SEC (~ 57 kDa). As the 100 kDa MWCO membrane was made from regenerated cellulose (Microcon), we sought to assess whether the nature of the membrane influences the recovery of the monomers. To that end, we compared aSyn monomer recovery through 100 kDa MWCO membranes made from regenerated cellulose (Microcon, used above) to that made from polyethersulfone (Vivaspin) (supplementary fig. 1C). As shown in supplementary fig. 1C, the efficiency of aSyn monomer recovery varied depending on the membrane composition. While regenerated cellulose membranes (Microcon) enabled the complete recovery of the monomers into the filtrate fraction, the polyethersulfone membrane (Vivaspin) retained approximately 20% of the protein in the retentate fractions. This analysis underscores the critical importance of evaluating the recovery efficiency of aSyn proteins prior to the use of spin filters to separate aSyn species or produce aggregate-free monomeric preparations.

Few studies have shown the existence of aSyn dimers in dynamic equilibrium with aSyn monomers (Marmolino *et al.* 2016; Coelho-Cerqueira *et al.* 2013). Although aSyn dimers have not been isolated as stable species, stable SDS-resistant dimers have been observed under conditions of oxidative stress that induces covalent chemical modification, for instance

dityrosine crosslinking, and in the presence of polyphenol-based small molecules (Souza *et al.* 2000; Masuda *et al.* 2006; Hashimoto *et al.* 1999). Therefore, we assessed whether the dimeric forms of aSyn would pass through the 100 kDa MWCO filters. Towards this goal, we generated stable disulfide-linked aSyn homodimers using recombinant aSyn proteins bearing a cysteine residue at the N- or C-terminus of the protein (M1C and A140C, supplementary fig. 1D and F). To determine whether the 100 kDa MWCO spin filters could separate monomers from dimers, an equimolar concentration mixture of WT aSyn monomers and homodimers was prepared and subjected to the same filtration conditions. Irrespective of the position of the cysteine mutation on the dimer (M1C or A140C homodimers), both monomers and dimers were recovered 100% in the filtrate fractions (supplementary fig. 1E and G), and no traces of the protein were observed in the retentate fractions.

Supplementary figure 2

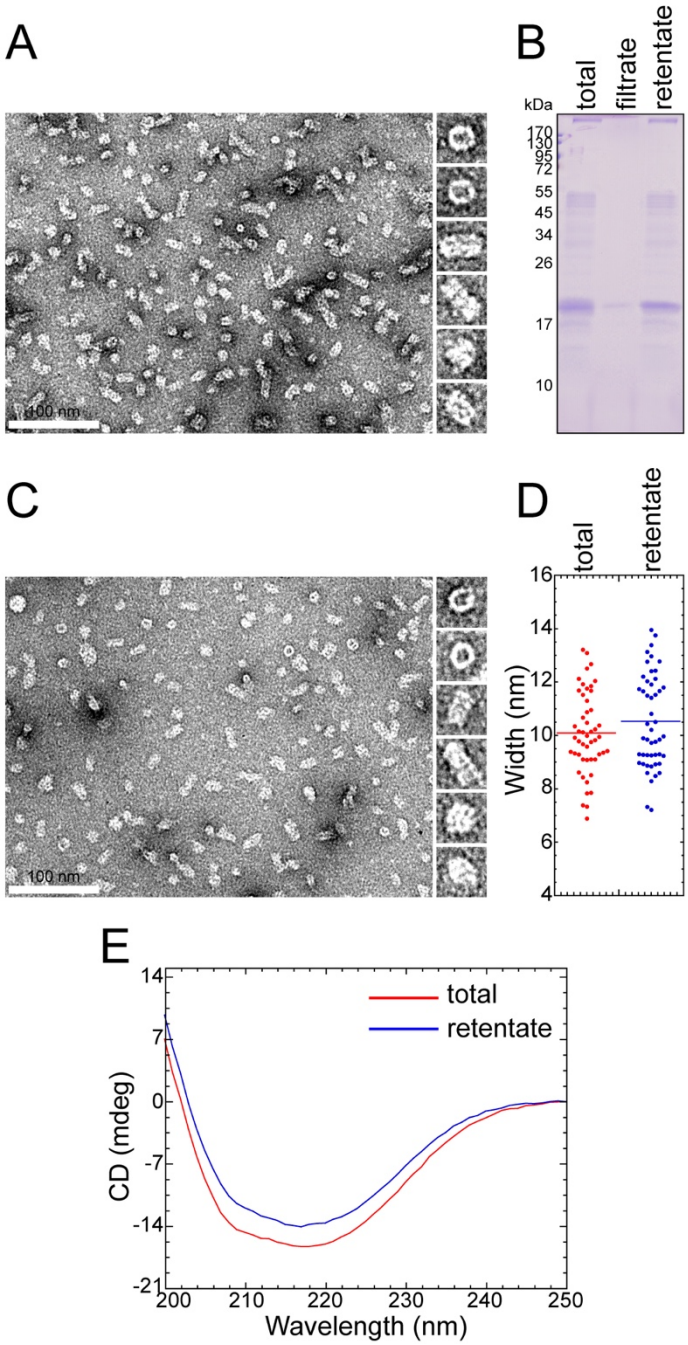


**Supplementary fig. 2:** aSyn oligomers recovered through 100 kDa MWCO filtration did not alter their secondary structure, size or morphology. A) EM image of total aSyn oligomers used for the filtration protocol and the montage showing the most represented oligomeric structures. B) SDS-PAGE analysis of the total, retentate and filtrate samples of aSyn oligomers. C) EM image of retentate aSyn oligomers recovered after the filtration protocol and the montage showing the most represented oligomeric structures. D) Width analysis of the total and retentate recovered oligomers. E) CD spectra of total and retentate recovered oligomers.

EM analysis of the oligomer preparations before applying the filtration protocol shows the appearance of annular, tubular and spherical morphologies (Supplementary fig. 2A) with diameters ranging between 6-14 nm (Supplementary fig. 2D). As expected, based on their size and dimensions, the aSyn oligomers did not pass through the 100 kDa MWCO filters and were recovered as retentate. The filtrate fraction showed negligible traces of aSyn monomers. Even when we sub-fractionate the oligomers into fractions of different size distributions ranging from 5-30 nm, we observed that all oligomers are retained and do not go through the 100 kDa MWCO filters. More importantly, EM analysis of the recovered oligomers revealed no significant changes in the size and morphology distribution of the aSyn oligomers (Supplementary fig. 2C). Comparison of the CD analysis of the original oligomer samples and the oligomers recovered in the retentate also showed no changes in their secondary structures. Previous sedimentation velocity and SEC studies have shown that these oligomeric preparations exhibit a size distribution with an average relative molecular mass that is slightly greater than 600 kDa (Lashuel *et al.* 2002).

Supplementary figure 3

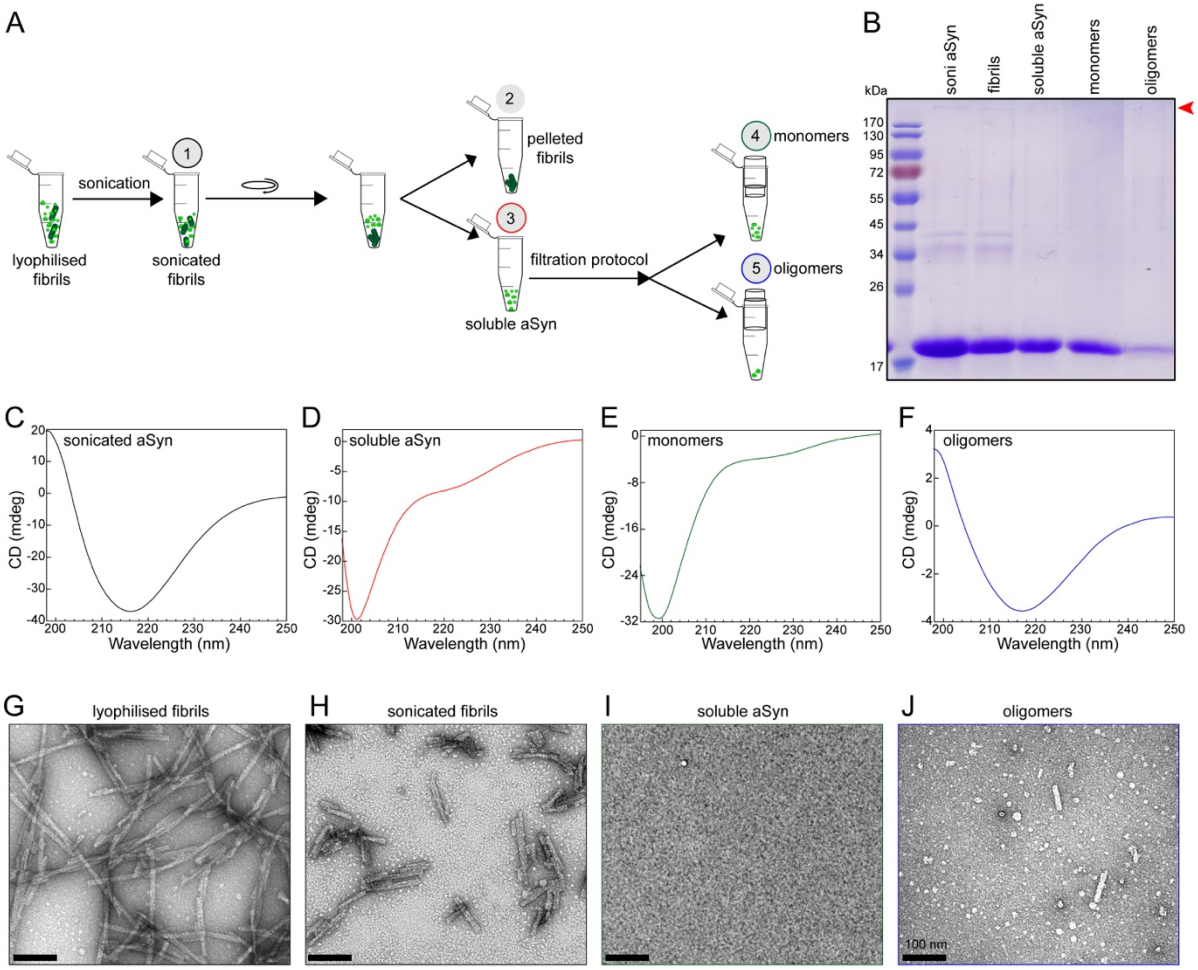


**Supplementary fig. 3:** A) Schematic depiction of the centrifugation-based filtration protocol characterization steps following sonication (referred to as sonicated fibrils) of the lyophilized fibrils. B) SDS-PAGE analysis of aSyn samples isolated from the different steps of the protocol. Red arrow head points the presence of SDS-resistant oligomeric band. C-F) CD spectra of sonicated fibrils (C), soluble aSyn (D), monomers (filtrate, E) and oligomers (retentate, F) in the samples. G-I) Representative electron micrograph images of lyophilized fibrils (G), sonicated fibrils (H), soluble aSyn (I), and oligomeric (retentate, J) samples.

**Assessing the effects of sonication on fibril stability and disassociation.**

Another potential application we envisioned for this protocol was to assess the amount of monomers/oligomers released during the preparation of aSyn PFFs for *in vitro* and *in vivo* seeding aggregation studies. Between laboratories, aSyn fibrils are transported in the frozen/freeze-dried form and are sonicated before their application for seeding studies. We have examined the effect of sonication on different batches of freshly prepared fibrils and revealed its varying effects on the release of soluble species. (Fig. 2F-H). Here, we investigated the same on the stability of lyophilized fibrils.

The same sample of lyophilized and resuspended aSyn fibril used in Fig. 5 was used in this experiment, but the centrifugation-based filtration protocol was applied following the sonication of fibrils, as illustrated in Supplementary fig. 3A. The SDS-PAGE analysis shown in Supplementary fig. 3 reveals the differences in the amount of aSyn species recovered in each step of the protocol. Supplementary fig. 3G and H show the EM images of the lyophilized aSyn fibrils, which were long and straight (Supplementary fig. 3G) and similar to that observed in the Fig. 5G; however, sonication produced fragmented fibrils with length distribution ranging from 100-200 nm. The sonicated fibrils (Supplementary fig. 3C) retain their β-sheet rich structure. As expected, the soluble aSyn species in the supernatant after centrifugation exhibited a CD spectra that reflects predominantly disordered conformations (Supplementary fig. 3D). aSyn oligomers were not easily visible by EM (Supplementary fig. 3I). However, upon filtration of the supernatant, we again observed nice separation of the unstructured monomers in the filtrate fraction (Supplementary fig. 3E) from the soluble oligomers with β-sheet structures in the retentate fraction (Supplementary fig. 3F). However, an important finding captured by the filtration protocol is that when compared to Fig. 5B, we see in Supplementary fig. 3B that there is an increase in the concentration of the the oligomeric sample recovered from the retentate fraction. This is also in agreement with the CD spectra which show a stronger CD signal (-3.8 CD (mdeg) on the y-axis, Supplementary fig. 3F) with a minimum at 218 nm compared to the weaker signal strength (at -1.2 CD (mdeg) on the y-axis, Fig. 5F), revealing an increase in the concentration of oligomers because of the effects of sonication on the lyophilized fibrils. Analogous to the oligomeric structures from Fig. 5I, the recovered aSyn sample (Supplementary fig. 3J) shows enrichment of spherical shaped oligomeric structures and the presence of very few short fragmented fibrils. This stress again the importance of this protocol in capturing the small differences on the level of different aSyn species, but these concentrations could be effective in bringing huge variations on the reproducibility of the experiments where these materials are used.

## References:


Bousset, L., Pieri, L., Ruiz-Arlandis, G. et al. (2013) Structural and functional characterization of two alpha-synuclein strains. *Nature Communications* **4,** 2575.

Chen, S. W., Drakulic, S., Deas, E. et al. (2015) Structural characterization of toxic oligomers that are kinetically trapped during alpha-synuclein fibril formation. *Proc Natl Acad Sci U S A* **112,** E1994-2003.

Coelho-Cerqueira, E., Carmo-Goncalves, P., Pinheiro, A. S., Cortines, J. and Follmer, C. (2013) alpha-Synuclein as an intrinsically disordered monomer--fact or artefact? *Febs j* **280,** 4915-4927.

Conway, K. A., Lee, S. J., Rochet, J. C., Ding, T. T., Williamson, R. E. and Lansbury, P. T., Jr. (2000) Acceleration of oligomerization, not fibrillization, is a shared property of both alpha-synuclein mutations linked to early-onset Parkinson's disease: implications for pathogenesis and therapy. *Proc Natl Acad Sci U S A* **97,** 571-576.

Danzer, K. M., Haasen, D., Karow, A. R., Moussaud, S., Habeck, M., Giese, A., Kretzschmar, H., Hengerer, B. and Kostka, M. (2007) Different species of alpha-synuclein oligomers induce calcium influx and seeding. *J Neurosci* **27,** 9220-9232.

Fares, M. B., Maco, B., Oueslati, A., Rockenstein, E., Ninkina, N., Buchman, V. L., Masliah, E. and Lashuel, H. A. (2016) Induction of de novo alpha-synuclein fibrillization in a neuronal model for Parkinson's disease. *Proc Natl Acad Sci U S A* **113,** E912-921.

Fenyi, A., Coens, A., Bellande, T., Melki, R. and Bousset, L. (2018) Assessment of the efficacy of different procedures that remove and disassemble alpha-synuclein, tau and A-beta fibrils from laboratory material and surfaces. *Scientific Reports* **8,** 10788.

Gao, X., Carroni, M., Nussbaum-Krammer, C. et al. (2015) Human Hsp70 Disaggregase Reverses Parkinson's-Linked alpha-Synuclein Amyloid Fibrils. *Mol Cell* **59,** 781-793.

Guo, J. L., Covell, D. J., Daniels, J. P. et al. (2013) Distinct alpha-synuclein strains differentially promote tau inclusions in neurons. *Cell* **154,** 103-117.

Hashimoto, M., Takeda, A., Hsu, L. J., Takenouchi, T. and Masliah, E. (1999) Role of cytochrome c as a stimulator of alpha-synuclein aggregation in Lewy body disease. *J Biol Chem* **274,** 28849-28852.

Lashuel, H. A., Petre, B. M., Wall, J., Simon, M., Nowak, R. J., Walz, T. and Lansbury, P. T., Jr. (2002) Alpha-synuclein, especially the Parkinson's disease-associated mutants, forms pore-like annular and tubular protofibrils. *J Mol Biol* **322,** 1089-1102.

Lorenzen, N., Nielsen, S. B., Buell, A. K. et al. (2014) The role of stable alpha-synuclein oligomers in the molecular events underlying amyloid formation. *J Am Chem Soc* **136,** 3859-3868.

Mahul-Mellier, A. L., Vercruysse, F., Maco, B., Ait-Bouziad, N., De Roo, M., Muller, D. and Lashuel, H. A. (2015) Fibril growth and seeding capacity play key roles in alpha-synuclein-mediated apoptotic cell death. *Cell Death Differ* **22,** 2107-2122.

Marmolino, D., Foerch, P., Atienzar, F. A., Staelens, L., Michel, A. and Scheller, D. (2016) Alpha synuclein dimers and oligomers are increased in overexpressing conditions in vitro and in vivo. *Mol Cell Neurosci* **71,** 92-101.

Masuda, M., Suzuki, N., Taniguchi, S., Oikawa, T., Nonaka, T., Iwatsubo, T., Hisanaga, S., Goedert, M. and Hasegawa, M. (2006) Small molecule inhibitors of alpha-synuclein filament assembly. *Biochemistry* **45,** 6085-6094.

Nasstrom, T., Fagerqvist, T., Barbu, M. et al. (2011) The lipid peroxidation products 4-oxo-2-nonenal and 4-hydroxy-2-nonenal promote the formation of alpha-synuclein

oligomers with distinct biochemical, morphological, and functional properties. *Free Radic Biol Med* **50,** 428-437.

Nasstrom, T., Wahlberg, T., Karlsson, M., Nikolajeff, F., Lannfelt, L., Ingelsson, M. and Bergstrom, J. (2009) The lipid peroxidation metabolite 4-oxo-2-nonenal cross-links alpha-synuclein causing rapid formation of stable oligomers. *Biochem Biophys Res Commun* **378,** 872-876.

Paslawski, W., Lorenzen, N. and Otzen, D. E. (2016) Formation and Characterization of alpha-Synuclein Oligomers. *Methods Mol Biol* **1345,** 133-150.

Pieri, L., Madiona, K. and Melki, R. (2016) Structural and functional properties of prefibrillar α-synuclein oligomers. *Scientific Reports* **6,** 24526.

Pieri, L., Madiona, K., Bousset, L. and Melki, R. (2012) Fibrillar alpha-synuclein and huntingtin exon 1 assemblies are toxic to the cells. *Biophys J* **102,** 2894-2905.

Souza, J. M., Giasson, B. I., Chen, Q., Lee, V. M. and Ischiropoulos, H. (2000) Dityrosine cross-linking promotes formation of stable alpha -synuclein polymers. Implication of nitrative and oxidative stress in the pathogenesis of neurodegenerative synucleinopathies. *J Biol Chem* **275,** 18344-18349.

Volles, M. J., Lee, S. J., Rochet, J. C., Shtilerman, M. D., Ding, T. T., Kessler, J. C. and Lansbury, P. T., Jr. (2001) Vesicle permeabilization by protofibrillar alpha-synuclein: implications for the pathogenesis and treatment of Parkinson's disease. *Biochemistry* **40,** 7812-7819.

Volpicelli-Daley, L. A., Luk, K. C. and Lee, V. M. (2014) Addition of exogenous alpha-synuclein preformed fibrils to primary neuronal cultures to seed recruitment of endogenous alpha-synuclein to Lewy body and Lewy neurite-like aggregates. *Nat Protoc* **9,** 2135-2146.